Neuroscience 344 (2017) 25–38

DEXAMETHASONE PREVENTS MOTOR DEFICITS AND NEUROVASCULAR DAMAGE PRODUCED BY SHIGA TOXIN 2 AND LIPOPOLYSACCHARIDE IN THE MOUSE STRIATUM

ALIPIO PINTO,[a] ADRIANA CANGELOSI,[b] PATRICIA A. GEOGHEGAN[b] AND JORGE GOLDSTEIN[a]*

[a] *Universidad de Buenos Aires, Consejo Nacional de Investigaciones Científicas y Técnicas (CONICET), Instituto de Fisiología y Biofísica "Houssay" (IFIBIO), Facultad de Medicina, Universidad de Buenos Aires, Argentina*

[b] *Centro Nacional de Control de Calidad de Biológicos (CNCCB), ANLIS "Dr. Carlos G. Malbrán", Buenos Aires, Argentina*

Abstract—Shiga toxin 2 (Stx2) from enterohemorrhagic *Escherichia coli* (EHEC) causes bloody diarrhea and Hemolytic Uremic Syndrome (HUS) that may derive to fatal neurological outcomes. Neurological abnormalities in the striatum are frequently observed in affected patients and in studies with animal models while motor disorders are usually associated with pyramidal and extra pyramidal systems. A translational murine model of encephalopathy was employed to demonstrate that systemic administration of a sublethal dose of Stx2 damaged the striatal microvasculature and astrocytes, increase the blood brain barrier permeability and caused neuronal degeneration. All these events were aggravated by lipopolysaccharide (LPS). The injury observed in the striatum coincided with locomotor behavioral alterations. The anti-inflammatory Dexamethasone resulted to prevent the observed neurologic and clinical signs, proving to be an effective drug. Therefore, the present work demonstrates that: (i) systemic sub-lethal Stx2 damages the striatal neurovascular unit as it succeeds to pass through the blood brain barrier. (ii) This damage is aggravated by the contribution of LPS which is also produced and secreted by EHEC, and (iii) the observed neurological alterations may be prevented by an anti-inflammatory treatment.

Key words: neuronal damage, inflammation, Blood–Brain Barrier, microvasculature, encephalopathy, Hemolytic Uremic Syndrome.

INTRODUCTION

Shiga toxin from enterohemorrhagic *Escherichia coli* (EHEC) causes hemorrhagic colitis and Hemolytic Uremic Syndrome (HUS) (Karmali, 2004), a triad of events that includes thrombocytopenia, microangiopathic hemolytic anemia and acute renal failure (Proulx et al., 2001).

Outbreaks by EHEC intoxication frequently occur worldwide in north and south hemispheres (Rivas et al., 2003; Grisaru et al., 2011). In 2011 an infrequent outbreak of foodborne hemorrhagic colitis took place in Germany and spread in Europe. About 3816 patients were intoxicated with Shiga toxin 2 (Stx2)-producing *Escherichia coli* (STEC) O104:H4 (Frank et al., 2011). Among them 845 developed HUS and 54 died (Bielaszewska et al., 2011; Frank et al., 2011; Scheutz et al., 2011). It is noteworthy that Argentina possesses the highest occurrence of HUS in the planet, with approximately 420 new cases reported every year and an incidence of 17/100.000 under the age of five (Rivas et al., 2003).

It has been reported that approximately 42% of the patients with HUS progress to any central nervous system (CNS) dysfunction (Gianantonio et al., 1973; Bale et al., 1980; Karmali et al., 1985). This turns to be significant because mortality rate derived from HUS ranges between 0–5% of the cases, and 7–40% when the CNS is involved (Upadhyaya et al., 1980; Sheth et al., 1986; Hahn et al., 1989). Moreover, CNS dysfunctions without or concomitantly with HUS symptoms have been reported on 9–15% of the affected patients (Brasher and Siegler, 1981; Karmali et al., 1985). It can be inferred from this a more prevailing local deleterious action of the toxin into the CNS than a collateral injury from affected organs like the kidney. To test this, Stx2 has been locally administered in the brain and consequently neuronal damaged was observed (Goldstein et al., 2007), probably through a Gb3 neuronal receptor for Stx2. Our group has localized the neuronal Gb3 receptor in different brain areas, including the striatum, and found that the expression of this receptor increased following Stx2 treatment (Tironi-Farinati et al., 2010). The striatum has been identified as one of the most vulnerable regions in the intoxication with STEC in patients (Obata, 2010).

Neurological symptoms in individuals include decerebrate posture, hemiparesis, ataxia, cranial nerve

*Corresponding author. Address: IFIBIO, Facultad de Medicina, Universidad de Buenos Aires, Paraguay 2155 piso 7, 1121 (CABA), Argentina.
E-mail addresses: jogol@fmed.uba.ar, jorgoldstein@gmail.com (J. Goldstein).

Abbreviations: CNS, central nervous system; EHEC, enterohemorrhagic *Escherichia coli*; GFAP, Glial fibrillary acidic protein; HUS, Hemolytic Uremic Syndrome; IOD, integral optical density; LPS, lipopolysaccharide; PBS, phosphate-buffered solution; STEC, Stx2-producing *Escherichia coli*; Stx2, Shiga toxin 2; VEGF, vascular endothelial growth factor.

http://dx.doi.org/10.1016/j.neuroscience.2016.12.036
0306-4522/

palsy, ophthalmological dysfunctions, hallucinations, seizures and changes in level of consciousness (from lethargy to coma) (Gianantonio et al., 1973; Cimolai et al., 1992; Hamano et al., 1993; Tapper et al., 1995). Similar symptoms were observed in mice that included lethargy, shivering, abnormal gait, hind limb paralysis, spasm-like seizure, reduced spontaneous motor activity, abnormal gait and pelvic elevation (Tironi-Farinati et al., 2013). Some of these symptoms are consistent with motor damage related to the pyramidal and extra pyramidal systems.

As it is known, EHEC not only secrete Stx2, but it also releases the outer membrane component lipopolysaccharide (LPS), an endotoxin that induces tissular production of a variety of inflammatory mediators when secreted in the gut. The LPS lipid A is the bioactive component of LPS, and its structure is highly conserved along *E. coli* strains. Moreover, the *E. coli* lipid A is a powerful activator of the innate immune system, and it contains two phosphate groups and six acyl chains composed by 12 or 14 carbons which is related with the infectivity of bacteria. In contrast, the lipid A of other bacteria out of *E. coli* contains four acyl chains and it does not activate the immune system (Alexander and Rietschel, 2001).

Accordingly, the injurious effects of these products have been reported *in vitro* and in various organs in individuals and in animal models (Zhang et al., 1997). However, few reports have investigated the deleterious contribution of LPS in EHEC-derived encephalopathies, a condition not fully determined in animal models nor considered in patients with HUS. In the present work an integrative study of the neuropathogenicity triggered by peripheral administration of sub-lethal Stx2 is carry out by immunofluorescence, physiological and behavioral means in the striatum of mice.

Therefore, the objective of this work was: (a) to study the contribution of LPS to pathogenicity in the neurovascular unit in striatal brain mice following systemic administration of a sub-lethal dose of Stx2, (b) to find a behavioral correlation respect the observed damage in the neurovascular unit, and (c) to determine whether these neurological alterations may be prevented by an anti-inflammatory treatment.

EXPERIMENTAL PROCEDURES

LD_{50} determination

Purified Stx2 was purchased at Phoenix Laboratory, Tufts Medical Center, Boston, MA, USA. The canonical Stx2 used was obtained from phage 933 W, named Stx2a (Plunkett et al., 1999). Stx2 was checked for LPS contamination by the limulus amoebocyte lysate assay. It contained < 10 pg LPS/ng of pure Stx2. The LPS used was from *E. coli* (L2880, Sigma, St. Louis, MO, USA). The amount of LPS used in this work was obtained from a measurement of Stx2 and LPS produced in the supernatant culture medium incubated with E. coli, and the ratio between Stx2: LPS yielded 1:800 (Goldstein et al., 2007).

The lethal effects of the Stx2 were characterized in mice ($n = 4$ per dose). As previously described (Tironi-Farinati et al., 2013), different amounts of Stx2 (5–0.44 ng per animal) or vehicle were administered intravenously (i.v.) to mice weighing about 20 g. Survival time was established when 100% of the animals survived at least 8 days after administration of Stx2. It was determined that the LD_{50} was 1.6 ng of toxin per animal, and with 1 ng (approximately 60% if this dose), mice survived even for more than 10 days (time when all survived animals were sacrificed). This amount was thus considered sub-lethal and it was selected for use in this study.

Dexamethasone survival assay

Six groups of mice ($n = 4$) were use to determine the protective effect of Dexamethasone against lethality by Stx2. Three groups of mice were endovenously treated with two lethal doses (LD) of Stx2 (3.2 ηg/mice), and the other three with vehicle saline solution (control). Two of these groups (one with two LD_{50} of Stx2 and the other with saline solution) were treated with two intraperitoneal (i.p.) administrations per day of saline solution (100 μl per injection), another two groups were treated with i.p. 7.5 mg/kg of Dexamethasone per day (3.75 mg per injection, data not shown) and the last two with i.p. 15 mg/kg of Dexamethasone per day (7.5 mg per injection). The assay lasted ten days. The number of animal's death per group and the day of the deaths were monitored.

Neurovascular toxicity and protection assay

Adult female Swiss mice (20 g) were housed in an air conditioned and light-controlled (lights on between 06:00 am and 06:00 pm) animal facility. Food and water were provided *ad libitum*. They were divided into four groups ($n = 8$) and subjected to the following i.v. treatments: LPS (800 ng); Stx2 (1 ng); LPS + Stx2 (1 ng Stx2 + 800 ng LPS); vehicle infusion (saline solution). Each animal received one i.v. dose in the lateral tail vein with 100 μl of solution. One half of the animals from each group ($n = 4$) were treated with 7.5 mg/kg i.p. Dexamethasone (100 μl per dose), twice a day for four days, while the other half of each group ($n = 4$) received 100 μl of i.p. saline solution, also twice a day for four days. All i.p. treatments (Dexamethasone or saline) started when they received their respective i.v. treatments (vehicle, LPS, Stx2 or Stx2 + LPS), and this day was referenced as day 0. All the animals were perfused on the fifth day (day of the first injection counted as day 1) as described in the following sentence.

Mice were anesthetized with pentobarbital (100 mg/kg) and perfused transcardially with 0.9% NaCl solution followed by 4% paraformaldehyde in 0.1 M phosphate-buffered solution (PBS) [fixative per animal weight (ml/g)] after 4 days of the respective treatment. Brains were removed from the skull and post-fixed with the same fixative solution for 2 h, and cryoprotected through a daily sequenced passage of increasingly concentrated of sucrose solutions (10%, 20% and 30%). Brain coronal sections (20-μm-thick) were cut with a

cryostat, maintained in a cryoprotectant solution (50% PBS 0.1 M, 30% Ethylene glycol, 20% Glycerol) at −20 °C, and subsequently processed for immunofluorescence microscopy.

The experimental protocols and euthanasia procedures were reviewed and approved by the Institutional Animal Care and Use Committee of the School of Medicine of Universidad de Buenos Aires, Argentina (Resolution N° 2437/2012). All the procedures were performed in accordance with the EEC guidelines for care and use of experimental animals (EEC Council 86/609).

Lectin histofluorescence

Six floating sections (the same number of sections was used for all immunofluorescence assays performed) for each treatment were subjected to Lycopersicum esculentum lectin histochemical marker to study the striatal endothelial cells. After several rinses with 10 mM PBS, sections were incubated with biotinylated lectin-10 μg/ml 0.3% Triton X-100 (Sigma, St. Louis, MO, USA) in the same buffer (4 °C for 24 h), and subsequently incubated with Alexa-488 Streptavidin (Invitrogen Molecular Probes, Carlsbad, California, USA (1:100) 0.3% Triton X-100 for 1 h at room temperature (RT), rinsed 3 times with 10 mM PBS and mounted on slides with a solution of glycerol and PBS 3:1 (sections for other immunofluorescence assays were also mounted in the same solution). Controls were performed using the same procedure but without adding the lectin protein. A green fluorescence filter was used to visualize brain striatum microvessels, and Adobe Photoshop software to assemble the images and obtain merged images (the same procedure was used for the other immunofluorescence assays).

Immunofluorescence

Brain floating sections were incubated with 0.1% Triton X-100 in the same buffer for one hour, followed by normal goat serum 10% (Sigma, St. Louis, MO, USA) with 0.3% Triton X-100 in PBS, also for one hour. After that sections were incubated with a primary antibody diluted in 10 mM PBS with 0.3% Triton X-100 at 4 °C for 48 h, as follows:

After several rinses with 10 mM PBS, brain floating sections were incubated with rabbit anti-vascular endothelial growth factor (VEGF, 1:500 – Santa Cruz Biotechnology, Santa Cruz, CA, USA), mouse anti-NeuN (1:500 – Millipore, Temecula, CA, USA), rabbit anti-glial fibrillary acidic protein (GFAP, 1:500 – Dako, Glostrup, Denmark), rabbit anti-microtubule-associated protein 2 (MAP2, 1:500 – Sigma, St. Louis, MO, USA), anti-Globotriaosylceramide (Gb3, 1:50 – Serotec, Kidington, UK), and with rabbit anti-Stx2 antibodies (1:500 – the anti-Stx2B IgG antibody was obtained as described by Parma et al. (2011)).

After several rinses with Triton X-100 0.025%, the sections were incubated with the secondary antibodies goat IgG anti-Rabbit Alexa Fluor 555 (Invitrogen Molecular Probes, Carlsbad, California, USA) diluted at 1:200 for anti-VEGF, GFAP, MAP2 or Stx2 immunofluorescences, with goat IgG anti-mouse/Texas Red (Amersham, GE, Piscataway, NJ, USA) diluted at 1:200 for anti-NeuN immunofluorescence, or with goat anti rat FIT-C (Jackson ImmunoResearch, West Grove, PA, USA) diluted at 1:200 for anti-Gb3 immunofluorescence in the same buffer with 0.3% Triton X-100 for 2 h (in anti-NeuN and VEGF immunofluorescences), or for 90 min (in anti-MAP2, Gb3 or Stx2 immunofluorescences) at room temperature. Finally, sections were rinsed with 10 mM PBS and mounted on slides. Controls were performed using the same procedure but without adding the primary antibody. A red fluorescence filter was used for visualization of immunofluorescence to detect VEGF, NeuN, GFAP, MAP2 or Stx2 proteins. A green fluorescence filter was used for visualization of immunofluorescence to Gb3 localization. With the purpose to observe the total cell distribution of Gb3 (that includes cell membrane and cytosolic Gb3 levels), mice brain slices were permeabilized with Triton X-100.

Evans Blue (EB) assay

For this test, we used the protocol described by del Valle et al. (2008). Mice were divided into eight groups as described in the Neurovascular Toxicity and Protection Assay, and after their respective treatment they were perfused transcardially with 0.9% NaCl solution followed by a solution with 4% paraformaldehyde and 1% EB in 0.1 M PBS [fixative per animal weight (ml/g)]. Brains were removed from the skull and post-fixed with the same fixative solution (without the EB staining) for 2 h and followed the same protocol as previously described. Brain coronal sections (25-μm-thick) were mounted on slides with a solution of glycerol and PBS 3:1.

Slides were examined under a confocal laser scanning biological microscope (Olympus FV10-ASW). EB staining was visualized by excitation with 543-nm laser beams (green zone) and visualized as red fluorescence. Controls were performed using the same procedure but without adding the EB staining on the fixative solution, to demonstrate that no autofluorescence is observed on these mice brain slices. The confocal parameters were set up in a way that no visible marks were observed on control brain slices. The same set parameters were used on all treated mice.

Merging images

The procedure described above was also employed to obtain merged images of GFAP and lectin immunofluorescence; VEGF and lectin immunofluorescence; Gb3 and GFAP immunofluorescence and/or Gb3 and NeuN immunofluorescence. The lectin histofluorescence protocol was always performed after GFAP or VEGF immunofluorescence, and the Gb3 protocol was always performed after GFAP and NeuN immunofluorescence. Hoechst 33342 (Sigma, St. Louis, MO, USA) was used (1 μg/ml 10 min RT) to show the cell nuclei of the brain

parenchyma. All analyses were carried out in the same comparable areas.

Analysis of micrographs

A total of 36 brain striatum micrographs per treatment were analyzed. The mean data were obtained from the measurement of the micrographs from the sections from the four independent brains per treatment. Micrographs were taken in the dorsal striatum to determine neurodegeneration (NeuN), endothelial damage (lectins), expression of vascular endothelial growth factor (VEGF), reactive astrocytes (GFAP), the Stx2 receptor expression (Gb3), Toxin permeability (Stx2) and The BBB permeability. A confocal laser scanning biological microscope (Olympus FV10-ASW) with a 40x objective lens was used. The images obtained were analyzed using the Image-J software (NIH). Two criteria were used to analyze endothelial damage: changes in glycocalyx expression in microvessels (as the number of glycocalyx particles bound to lectins) and density of microvessels (as the percentage of area occupied by microvessels). The particles analyzed were quantified by conversion into 8-bit and contrasted against the background using the threshold tool. Moreover, objects with an area less than 10 μm^2 were excluded to avoid quantified dots from the background (Pinto et al., 2013; Ferreira and Rasband, 2010). In addition, VEGF-immunopositive particles were quantified as described above. Acquired images were opened using Adobe Photoshop CS software to determine neurodegeneration, and nuclei with normal phenotype were quantified and painted to avoid errors. These data were represented as the percentage of degenerated nuclei in respect of total nuclei per micrograph. The same technique was used to determine the BBB permeability to Stx2 and the Gb3 expression. The ROI Manager analyze tool on Image-J software was employed to quantify the expression of GFAP to determine reactive astrocytes, MAP2 and BBB permeability. For this, the color channels of the micrographs opened with this software were split, and the area of the ones with the red color channel (now on an 8bit gray scale format) was selected. The other channels (green and blue) were discarded. The values from the background observed on all negative control micrographs were subtracted from the mice treated micrographs.

Open field test

To evaluate locomotor activity, animals were exposed to an open field test. The open field used in this experiment consisted of a wooden apparatus with 50 cm high, 50 cm wide, and 39 cm deep arena with black walls and a brown floor divided equally into nine squares by white lines. Each animal was gently placed at the center of the open field and the number of line crossings was measured manually during each minute, in a 5-min test session. In order to remove any olfactory cues, the apparatus was cleaned with 70% isopropylic alcohol after each test.

Statistical analysis

The data are presented as mean ± SEM. In the case of different toxicity-treated groups and their respective controls at one-time point (4 days of treatment) in the neurovascular toxicity and protection assays, statistical significance was performed using a one-way analysis of variance (ANOVA) followed by Tukey's multiple comparison test between the 4 i.v. treatments (vehicle, LPS, Stx2 and Stx2 + LPS). In the case of comparison of different treatment groups and their respective controls when challenged with i.p. Dexamethasone or saline solution, a two-way analysis of ANOVA was used followed Bonferroni post hoc test (GraphPad Prism 4, GraphPad Software, Inc.) in the following experiments: lectin histofluorescence, immunofluorescence methods, EB assay (Sample size = 36, Degrees of freedom = 35) and Open field test (sample size = 8, Degrees of freedom = 7). The criterion for significance was $p \leqslant 0.05$ for all the experiments.

In addition, another set of statistical tests were assayed with the purpose of further analyzing the assumptions of two way variances. Firstly, the Shapiro–Wilks normality test was applied and it was verified that the dependent variable followed an approximately normal distribution. Then, the Levene test was applied to evaluate the variances homogeneity; $p < 0.05$ was obtained, which indicates no variances homogeneity. Two-way ANOVA (one factor: the 4 e.v. treatments, vehicle, LPS, Stx2 and Stx2 + LPS. The second factor: without and with Dexamethasone) supposed unequal variances. The Games-Howell test is designed for unequal variances. In addition, the T3 Dunnet test is used alternatively to the Games-Howell test when it is fundamental to keep the control over the significance level between various tests. The Games-Howell and T3 Dunnet tests showed significant differences between all groups at the level of 0.05, in the following experiments: lectin histofluorescence, immunofluorescence methods, EB assay (Sample size = 36, Degrees of freedom = 35) and Open field test (sample size = 8, Degrees of freedom = 7). These statistical findings coincided with the significant differences found in Tukey and Bonferroni post hoc tests.

The number of animals used in this work (A total of 128 animals: $n = 4$ in neurovascular protection and EB assay; $n = 8$ in Open field test) yielded error bars with low dispersion and therefore it was not necessary to subject additional animals and/or brain sections to these treatments.

RESULTS

Dexamethasone protects mice from Stx2 lethality

A survival curve was done to determine the protective effect of Dexamethasone challenged against two lethal doses 100% (DL_{100}) of Stx2. All vehicle-treated mice (control) survived the ten days of screening. In contrast, all mice administered e.v. with Stx2 and i.p. with saline solution were found dead at day five (Fig. 1). This was the same for mice treated with e.v. Stx2 and i.p. 7.5 mg

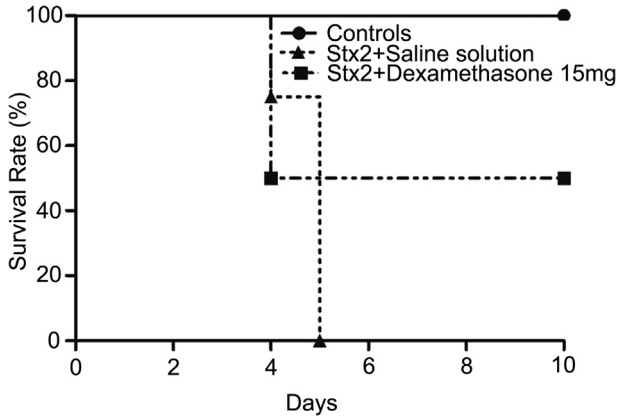

Fig. 1. Survival curve. The survival effect of Dexamethasone was challenged against two DL_{100} of Stx2 in mice (Stx2 + Dexamethasone 15 mg).

of Dexamethasone per day (data not shown). However the administration of e.v. Stx2 and i.p. 15 mg of Dexamethasone per day indeed protected from dead in 50% of mice (Fig. 1).

Sub-lethal dose of Stx2

As it was observed that the administration of 2 LD_{100} of Stx2 caused the death of mice after 5 days, it was determined to use in the following experiments a sub-lethal dose of Stx2, by which the administration of the toxin did not cause any death (Tironi-Farinati et al., 2013) and allowed to study the pathogenicity caused by Stx2 in the neurovascular unit in striatal brain mice. This strategy resembles those patients intoxicated with EHEC but succeeded to survive, although they may remain with neurological abnormalities. In addition, the contribution of LPS in the pathogenicity caused by Stx2 was also carried on.

Intravenous administration of a sublethal dose of Stx2 changes the profile of microvessels, LPS exacerbates it and Dexamethasone recovers microvessel integrity in the brain striatum

Lectins are non-immune proteins that bind with high affinity to specific N-acetyl-D-glucosamine and poly-N-acetyl lactosamine sugar residues of endothelial plasma membrane glycocalyx (Mazzetti et al., 2004) and they are useful to study the microvasculature profile. Therefore, lectins were used to detect the changes in the microvasculature after 4 days of treatment. Saline-treated control mice (vehicle) showed a continuous lectin fluorescence binding throughout all microvessel cell membranes (Fig. 2A). Vehicle microvessels were found well preserved with defined edges. In contrast to this treatment with the toxins (Stx2 + LPS) resulted to produce a discontinuous lectin fluorescence binding distributed in patches with poorly defined edges (Fig. 2B–D). No lectin fluorescence binding was detected when lectin incubation was omitted (Fig. 2I).

All the observed changes in the microvasculature profile were confirmed by morphometric analysis: the number of positive glycocalyx-particles bound to fluorescence lectins (Fig. 2J) and the percentages of microvessels that occupy a determined area (Fig. 2K) were determined. As a result of discontinuous microvessel glycocalyx distribution, the maximal increase in the number of positive glycocalyx particles bound to fluorescence lectins per field was significantly observed in Stx2 + LPS-treated mice (122.62 ± 3.07, followed by Stx2-treated ones (105.86 ± 4.70), and then LPS-treated mice (59.77 ± 4.05), in comparison with vehicle-treated mice (35.56 ± 2.88), $p \leqslant 0.05$ (Fig. 2J). Conversely, microvessels from LPS-treated mice occupied a minor area in the striatum per observed field in comparison with vehicle-treated mice; microvessels from Stx2-treated mice occupied a minor area in comparison to LPS- and vehicle-treated groups, and microvessels from the co-administration of Stx2 and LPS (Stx2 + LPS) occupied the smallest area of all treatments: 18.44 ± 0.97% (vehicle); 9.92 ± 0.57% (LPS); 5.50 ± 0.79% (Stx2); 3.61 ± 0.53% (Stx2 + LPS); $p \leqslant 0.05$ (Fig. 2K). Treatment with Dexamethasone partially recovered glycocalyx distribution in

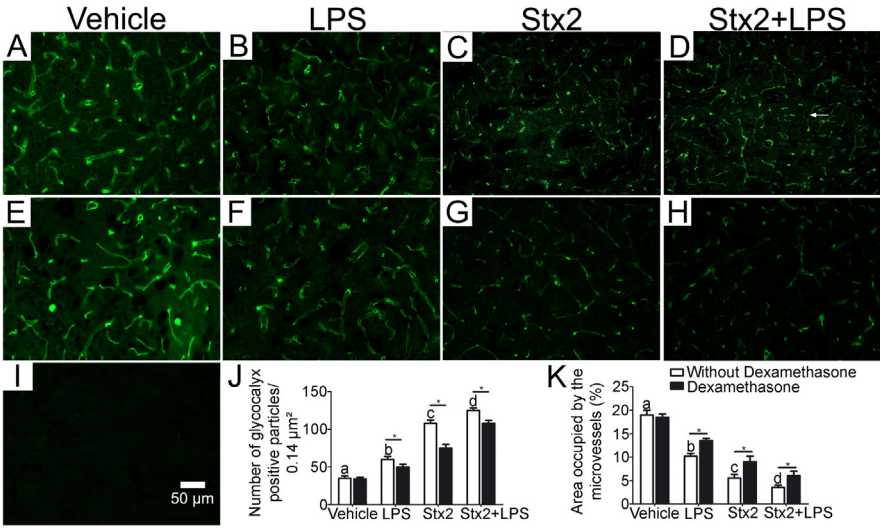

Fig. 2. Changes in the distribution of glycocalyx particles bound to fluorescent lectins in the microvasculature of mice striatum. Treatment without Dexamethasone (A–D); treatment with Dexamethasone (E–H). (A, E) Show the microvasculature profile in the control groups (vehicle treatment); (B, F) LPS treatment; (C, G) Stx2 treatment; (D, H) Stx2 + LPS treatment. Arrow shows microvessels devoid of glycocalyx particles bound to fluorescent lectins (D). The number of positive glycocalyx particles for all treated groups is shown (J). Microvessel density for all treated groups is shown (K). Negative control (I). Different letters (a, b, c or d) above the columns indicate a significant difference between the four different e.v.-treated groups without Dexamethasone treatment ($p \leqslant 0.05$). *Significant difference between the Dexamethasone-treated group with the same e.v.-treated group but without Dexamethasone ($p \leqslant 0.05$). Data are mean ± SEM. The scale bar in I applies to all micrographs.

microvessels by reducing the number of discontinuous microvessel glycocalyx particles bound to fluorescent lectins in all-treated mice by: 16.35% in LPS; 30% in Stx2; 13.67% in Stx2 + LPS-treated mice, except in vehicle-treated one (Fig. 2E–H), $p \leqslant 0.05$ (Fig. 2J). Microvessel density was increased in all-treated mice but not in vehicle-treated mice (Fig. 2E–H): 32.96% in LPS; 61.45% in Stx2; 66.20% in Stx2 + LPS-treated mice, $p \leqslant 0.05$ (Fig. 2K).

Sublethal doses of Stx2 + LPS and Stx2 inhibit the expression of VEGF while Dexamethasone restores VEGF immunoexpression in striatal microvessels

Following the observation that Stx2 + LPS and Stx2 changed the profile of microvessels, it was postulated that they could also change the expression of VEGF, an angiogenic growth factor that may appear under regenerative processes. An anti-VEGF antibody was employed to evaluate whether LPS, Stx2 or Stx2 + LPS changed the expression of VEGF in striatal microvessels. While a complete inhibition of VEGF immunoexpression was observed in Stx2- and Stx2 + LPS-treated mice (Fig. 3A–D, J), a significant decrease in VEGF immunoexpression (expressed as number of particles per area) was observed in LPS-treated mice in comparison with the vehicle one: 24.44 ± 5.85 (LPS) vs 61.37 ± 3.78 (vehicle), $p \leqslant 0.05$ (Fig. 3J). Conversely, the treatment with Dexamethasone succeeded to restore the immunoexpression of VEGF in microvessels of LPS, Stx2 and Stx2 + LPS-treated mice (Fig. 3F–H), to 130.22%, 52.03% and 29.81% respectively, in comparison to vehicle-treated mice, $p \leqslant 0.05$ (Fig. 3J). No immunofluorescence pattern was observed by the omission of primary antibody (Fig. 3I).

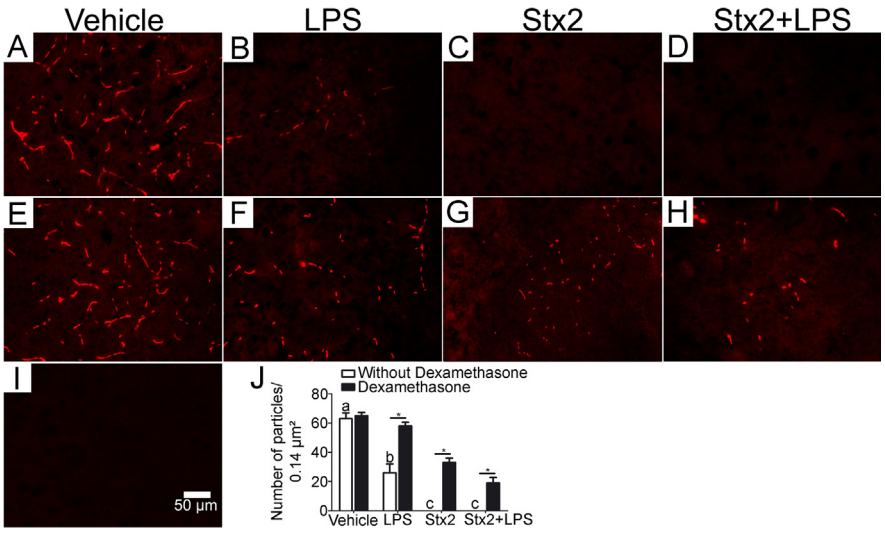

Fig. 3. Changes in immunofluorescence to VEGF. Treatment without Dexamethasone (A–D); treatment with Dexamethasone (E–H). (A, E) Show the VEGF profile in the control groups (vehicle treatment); (B, F) LPS treatment; (C, G) Stx2 treatment; (D) H, Stx2 + LPS treatment. Negative control (I). Different letters (a, b or c) above the columns indicate a significant difference between the four different e.v.-treated groups without Dexamethasone treatment ($p \leqslant 0.05$). *Significant difference between the Dexamethasone-treated group with the same e.v.-treated group but without Dexamethasone ($p \leqslant 0.05$). Data are mean ± SEM. The scale bar in I applies to all micrographs.

Intravenous administration of a sublethal dose of Stx2 increases BBB permeability, the combination with LPS exacerbates this effect and Dexamethasone decreases the BBB permeability

The changes on the observed microvessel profile following Stx2 and/or Stx2 + LPS treatments were determined by morphological means (see Fig. 2) suggesting that BBB disruption might occurred in the striatum (Fig. 4Y). Therefore, the Evans Blue Assay was employed to determine whether LPS, Stx2 or Stx2 + LPS changed the BBB permeability. The Evans Blue is a compound that binds to plasma proteins by which under physiological conditions may not cross the BBB (del Valle et al., 2008). Quantification of Evans Blue levels on the cerebral parenchyma was measured by integral optical density (IOD). Negative controls were obtained by not adding Evans Blue and no fluorescence was detected (Fig. 4–1). A significant increase on BBB permeability was observed in LPS- (27.98 ± 3.72), Stx2- (45.00 ± 1.89) and Stx2 + LPS-treated mice (75.11 ± 3.25) compared with the control ones (vehicle, no permeability to Evans Blue) (Fig. 4A–D, Z); the significant differences found in all toxin groups ($p \leqslant 0.05$, Fig. 4Z), suggested that LPS exacerbated the Stx2 effects since maximal BBB permeability was observed after Stx2 + LPS administration (Fig. 4D, Z). On the other hand, after 4 days, Dexamethasone treatment reduced completely the BBB permeability in LPS-treated mice, and it reduced by 51.13% in Stx2- and 57.40% in Stx2 + LPS-treated mice. No change in BBB permeability was observed in vehicle-treated mice following Dexamethasone treatment ($p \leqslant 0.05$) (Fig. 4M–P, Z).

Sublethal dose of Stx2 causes reactive astrocytes, and this effect is exacerbated when LPS is combined, while Dexamethasone reduces the number of reactive astrocytes

GFAP is an astrocytic cytoskeletal protein that is increased (reactive astrocyte) following an ample variety of brain injuries. Accordingly, GFAP expression levels were quantified by IOD values to determine whether systemic administration of LPS, Stx2 and/or Stx2 + LPS caused reactive astrocytes (Fig. 5J). No immunofluorescence was observed in negative controls by omitting primary antibody (Fig. 5I). After 4 days of treatment the LPS administration significantly increased the expression of GFAP respect the vehicle, Fig. 5A, B, J) while Stx2 administration increased the

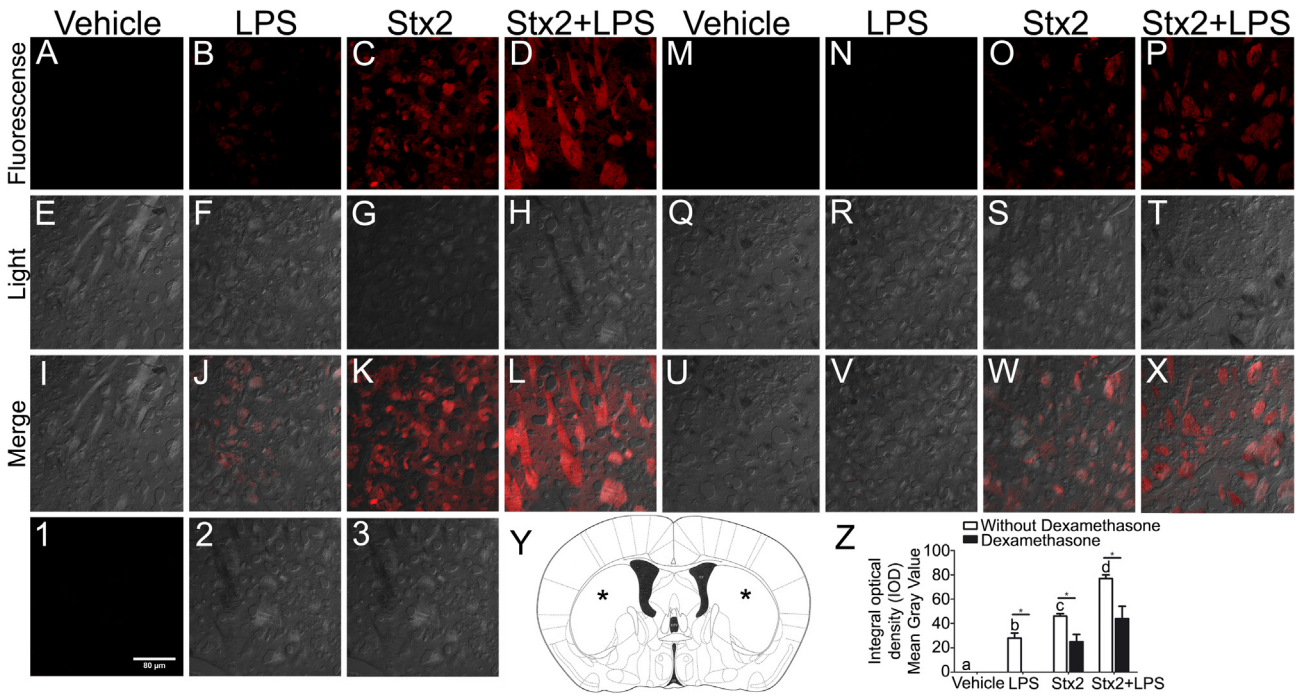

Fig. 4. Increase of BBB permeability. Evans Blue staining was employed to show permeability of the BBB (A–X). Treatments without Dexamethasone (A–L) include: vehicle (A, E, I), LPS (B, F, J), Stx2 (C, G, K) and Stx2 + LPS (D, H, L). Treatments with Dexamethasone (M–X) include: vehicle (M, Q, U), LPS (N, R, V), Stx2 (O, S, W) or Stx2 + LPS (P, T, X). Negative controls by not adding Evans Blue: fluorescence microscopy (1), light microscopy (2) and merge between fluorescence and light microscopy (3). Striatum (Y). Quantification of BBB permeability by Evans Blue fluorescence staining in the striatum (Z). Different letters (a, b, c or d) above the columns indicate a significant difference between the four different e.v.-treated groups without Dexamethasone treatment ($p \leqslant 0.05$). *Significant difference between the Dexamethasone-treated group with the same e.v.-treated group but without Dexamethasone ($p \leqslant 0.05$). Data are mean ± SEM. The scale bar in 1 applies to all micrographs.

expression of GFAP respect LPS and the control (Fig. 5A–C, J). Co-administration of Stx2 + LPS resulted to maximally increased GFAP expression in all other groups: 46.10 ± 1.68 (vehicle); 56.21 ± 2.75 (LPS); 64.01 ± 2.10 (Stx2); 75.36 ± 2.11 (Stx2 + LPS) (Fig. 5A–D, J), while Dexamethasone administration succeeded to significantly decrease the expression of GFAP in all treated groups except the control one: 13.9% LPS; 11.86% Stx2; 12.57% Stx2 + LPS (Fig. 5E–H, J): $p \leqslant 0.05$ between toxin-treated and control groups and $p \leqslant 0.05$ between Stx2 and Stx2 + LPS treatments.

Sublethal Stx2 produces neurodegeneration, LPS exacerbates it and Dexamethasone is neuroprotector

Anti-NeuN antibody was employed to determine whether systemic administration of LPS, Stx2 or Stx2 + LPS caused neurodegeneration. A conserved and homogeneous nuclear immunofluorescence pattern for Neu-N confirmed healthy neurons (Fig. 6A) while a perinuclear pattern or nuclear dotted immunofluorescence showed a neurodegenerative phenotype (Fig. 6D, J). No immunofluorescence was observed in negative controls by omitting primary antibody (Fig. 6I). A significant increase of neuronal nuclei with abnormal phenotype showed neurons in a degenerative condition 4 days after the administration of LPS (15.05 ± 1.80), Stx2 (29.48 ± 0.95) or Stx2 + LPS (35.46 ± 1.75) (Fig. 5A–D), in comparison with the vehicle (1.54 ± 0.98), ($p \leqslant 0.05$). As observed, maximal increase of degenerated neurons was observed in Stx2 + LPS-treated group (Fig. 6D, K). Dexamethasone administration resulted to decrease the number of degenerative cells in the three toxin-treated groups by 33.23% (LPS-), 42.3% (Stx2-) and 44.2% Stx2 + LPS), while no significant change was observed in controls, ($p \leqslant 0.05$), (Fig. 6E–H, K).

Intravenous administration of a sublethal dose of Stx2 decreases the expression of MAP2, and the combination with LPS exacerbates this effect. Dexamethasone increases MAP2 expression

Microtubule-associated protein 2 (MAP2) is a cytoskeletal neuronal marker specifically found in neuronal bodies and postsynaptic structures related to dendritic bodies and synaptic plasticity. An anti-MAP2 antibody was employed to determine whether systemic administration of LPS, Stx2 or Stx2 + LPS changes its expression. Quantification of MAP2 levels was measured by IOD values (Fig. 7J). After 4 days MAP2 immunofluorescence was decreased following Stx2 (19.50 ± 1.88) and Stx2 + LPS (14.25 ± 0.49) administrations in comparison to the vehicle (45.05 ± 2.77), $p \leqslant 0.05$ (Fig. 7A, C, D). No significant differences were observed between vehicle and LPS (38.21 ± 3.16) treatments, $p \leqslant 0.05$ (Fig. 7A, B, J). As

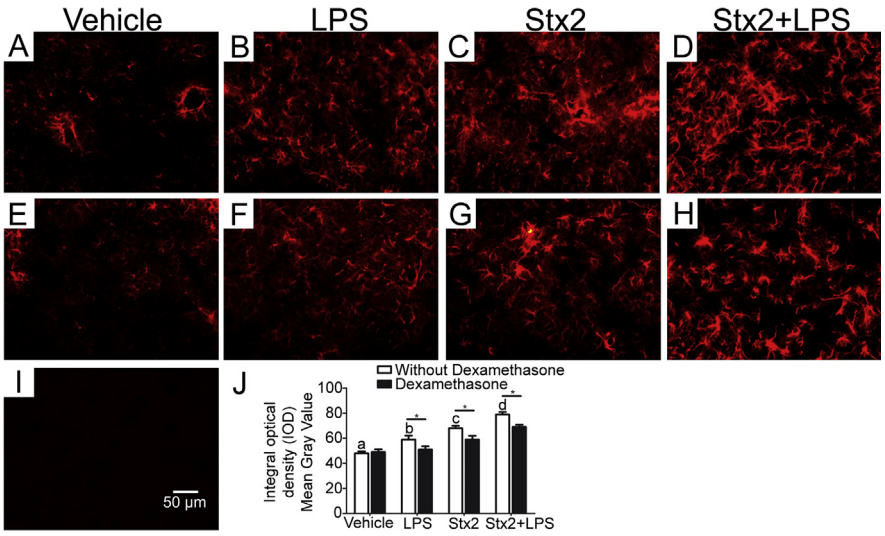

Fig. 5. Stx2 and Stx2 + LPS produce reactive astrocytes. Treatment without Dexamethasone (A–D); treatment with Dexamethasone (E–H). Immunofluorescence using an anti-GFAP antibody was employed to show reactive astrocytes. (A, E) vehicle-treated astrocytes; (B, F) LPS-treated astrocytes; (C, G) Stx2-treated astrocytes; (D, H) Stx2 + LPS-treated astrocytes. Quantification of reactive astrocytes (J) under all treatments. (I) Negative control by not adding the primary antibody. Different letters (a, b, c or d) above the columns indicate a significant difference between the four different e.v.-treated groups without Dexamethasone treatment ($p \leqslant 0.05$). *Significant difference between the Dexamethasone-treated group with the same e.v. treated group but without Dexamethasone ($p \leqslant 0.05$). Data are mean ± SEM. The scale bar in I applies to all micrographs.

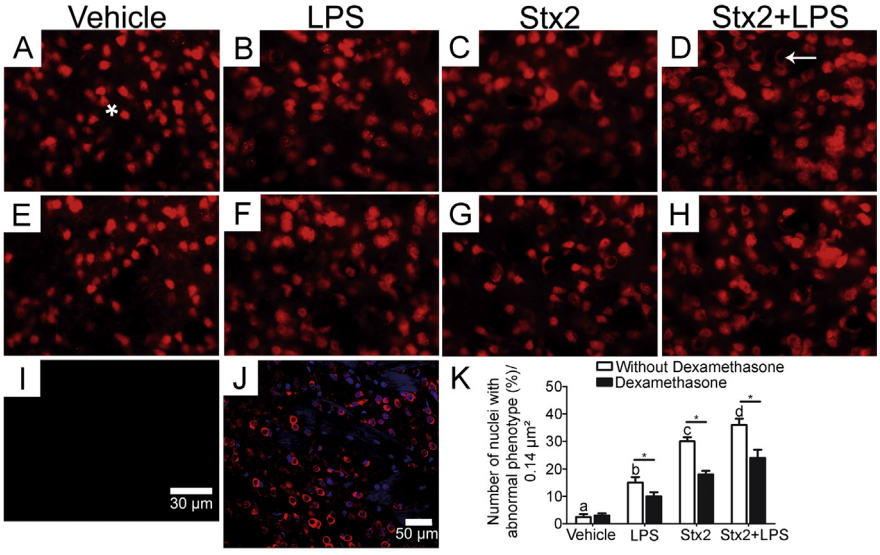

Fig. 6. Changes of NeuN expression. Treatment without Dexamethasone (A–D); treatment with Dexamethasone (E–H). Micrographs show immunofluorescence staining for NeuN in the nucleus of neurons with anti-NeuN. (A, E) Vehicle; (B, F) LPS; (C, G) Stx2; (D, H) Stx2 + LPS. Arrows show nuclei of degenerating neurons (D); asterisk shows normal nuclei of neurons (A). Negative control by not adding the primary antibody (I). Merge between a NeuN micrograph (red) and Hoechst one (blue) showing the localization of perinuclear NeuN abnormal neurons and nuclear Hoechst (J). Dexamethasone decreases the percentage of degenerative neurons (K). Different letters (a, b, c or d) above the columns indicate a significant difference between the four different e.v.-treated groups without Dexamethasone treatment ($p \leqslant 0.05$). *Significant difference between the Dexamethasone-treated group with the same e.v.-treated group but without Dexamethasone ($p \leqslant 0.05$). Data are mean ± SEM. The scale bar in I applies to A–H micrographs. (For interpretation of the references to colour in this figure legend, the reader is referred to the web version of this articl.)

observed, the maximal decrease on its expression was observed after Stx2 + LPS administration (Fig. 7D, J). Treatment with Dexamethasone partially recovered MAP2 immunofluorescence in Stx2- (84.3%) and in Stx2 + LPS-treated mice (75.79%), $p \leqslant 0.05$ (Fig. 7E, G, H, J). No immunofluorescence to MAP2 immunoreactivity was observed in negative controls by omitting primary antibody (Fig. 7I).

Intravenous administration of a sublethal dose of Stx2 increases the expression of its receptor Gb3 and the combination with LPS exacerbates this expression. Dexamethasone decreases the expression of Gb3

An anti-Gb3 antibody was employed to determine whether systemic administration of LPS, Stx2 or Stx2 + LPS increases the expression of Gb3 receptor. The number of immunopositive cells for Gb3 was counted for every treatment (Fig. 8L). A significant increase in the number of Gb3-positive cells were found after 4 days of treatment following LPS, Stx2 and Stx2 + LPS treatments (vehicle 20.65 ± 4.70; LPS 47.89 ± 5.39; Stx2 73.71 ± 5.88; Stx2 + LPS 103.52 ± 7.80), $p \leqslant 0.05$ (Fig. 8A–D, L). Maximal increase observed in Gb3-immunopositive neurons was found in Stx2 + LPS-treated mice in comparison to the Stx2- or LPS-treated ones (Fig. 8B–D, L). The significant differences between the Gb3 expressions found in all toxins groups suggested that LPS plays an important role in the receptor expression. The precise distribution of it was confined to neurons (Fig. 8K) and not to astrocytes, then the deleterious effects of Stx2 observed in neurons may occur directly through Gb3 (Fig. 8J, K). Dexamethasone administration significantly reduced the number of Gb3-positive neurons in all treated mice except in the control group (37.28% LPS; 23.89% Stx2; 21.55% Stx2 + LPS), $p \leqslant 0.05$ (Fig. 8E–H, L). No immunofluorescence to Gb3 immunoreactivity was observed in negative controls by omitting primary antibody (Fig. 8I).

Stx2 is immunolocalized in striatal parenchyma cells and when Stx2 is combined with LPS more Stx2-immunopositive cells are found. Dexamethasone decreases Stx2-immunopositive cells

Intravenous administration of LPS, Stx2 and Stx2 + LPS was employed to determine whether Stx2 succeeds to pass through the BBB and also whether the LPS contribution increases the BBB permeability to Stx2. Immunolocalization of Stx2 was observed in striatal cells (Fig. 9C, D, G, H, J). This event suggested that the BBB might be permeable to Stx2 (Fig. 9C, D). Immunopositive cells for Stx2 in vehicle and LPS treatments were absent (Fig. 9A, B). No immunofluorescence was observed by omitting primary antibody (Fig. 9I). Stx2 + LPS treatment significantly increased the number of immunopositive cells for Stx2 in comparison to the treatment with Stx2 alone (324.76 ± 25.12 vs 256.28 ± 9.56 respectively, $p \leqslant 0.05$, Fig. 9C, D, J). This was evidenced in the increased number of Stx2-positive cells (Fig. 9J) and in the expression levels of Stx2 inside the cells measured by IOD (254.54 ± 8.65, Stx2; 325.54 ± 24.24, Stx2 + LPS, $p \leqslant 0.05$, Fig. 9K). Dexamethasone treatment significantly reduced the number of Stx2-immunopositive cells in Stx2-treated mice by 28.05% and in Stx2 + LPS-treated mice by 26.16%, $p \leqslant 0.05$, while the expression levels of Stx2 in Stx2- and Stx2 + LPS-treated mice were reduced by 26.20% and 26.07% respectively, $p \leqslant 0.05$ (Fig. 9J, K). These results suggested that the BBB permeability to Stx2 in Stx2 and Stx2 + LPS were decreased when were challenged with Dexamethasone (Fig. 9E–H, J, K).

Intravenous administration of a sublethal dose of Stx2 decreases locomotor activity, LPS exacerbates the Stx2 effect while Dexamethasone partially recovers locomotor activity

To determine whether the neurovascular damage caused by the toxins may alter locomotor behavior an Open Field test was performed. This test evaluates motor activity by measuring the number of line crossings at the Open Field arena. Vehicle-treated mice showed a high locomotor activity, which was significantly decreased in Stx2- and Stx2 + LPS-treated mice (141.61 ± 16.55, vehicle; 114.59 ± 13.95, LPS; 85.83 ± 7.95, Stx2; 46.62 ± 12.20, Stx2 + LPS; $p \leqslant 0.05$, Fig. 10). Maximal locomotor decrease was observed following Stx2 + LPS administration, while no significant differences were observed between control and LPS treatments (Fig. 10). Dexamethasone administration significantly improved the locomotor activity after 4 days of treatment in Stx2-treated mice by 25.9%, while it was maximally improved in the Stx2 + LPS-treated mice by 103.73%, $p \leqslant 0.05$ (Fig. 10).

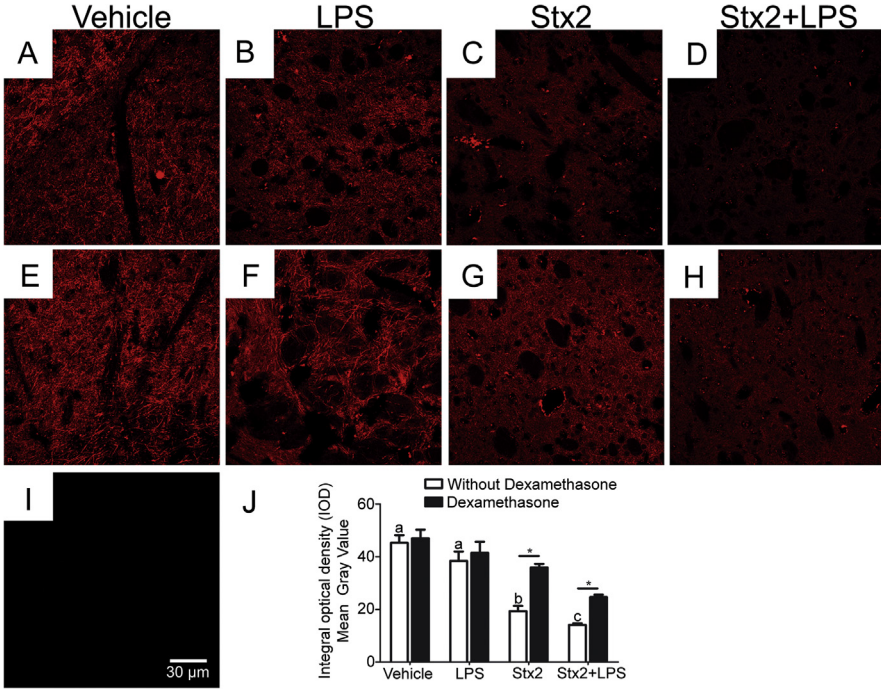

Fig. 7. Changes in MAP2 expression. Treatment without Dexamethasone (A–D); treatment with Dexamethasone (E–H). Micrographs show immunofluorescence staining for MAP2 in neuronal projections with anti-MAP2. (A, E) Vehicle; (B, F) LPS; (C, G) Stx2; (D, H) Stx2 + LPS. (I) Negative control by not adding the primary antibody. Dexamethasone increases the levels of MAP2 immunofluorescence expression (J). Different letters (a, b, or c) above the columns indicate a significant difference between the 4 different e.v.-treated groups without Dexamethasone treatment ($p \leqslant 0.05$). *Significant difference between the Dexamethasone-treated group with the same e.v.-treated group but without Dexamethasone ($p \leqslant 0.05$). Data are mean ± SEM. The scale bar in I applies to all micrographs.

DISCUSSION

It has been reported that systemic infection of Stx2 produced by EHEC can lead to an encephalopathy. Neurological disorders found in children affected with HUS are one of the major causes of mortality (Upadhyaya et al., 1980; Sheth et al., 1986; Hahn et al., 1989). To study these disorders various animal models were proposed to investigate these neurological symptoms (Fujii et al., 1996; Kita et al., 2000; Mizuguchi et al., 2001). In our murine model, we tried to extrapolate the neurological damage found in patients by a systemic administration of Stx2 and/or Stx2 together with LPS, as EHEC not only secrete Stx2 but also LPS is absorbed in the gut, a structural component present in the outer membrane of all Gram-negative bacteria (Koster et al., 1978; Bitzan et al., 1991; Louise and Obrig, 1992). The finding of Stx2 cytotoxicity enhancement by LPS resulted to be consistent with previous reports in which *in vitro* incubation of Stx2 with LPS in human umbilical vein endothelial cell culture resulted to increase the cytotoxic effect in comparison with the Stx2 alone (Louise and Obrig, 1992),

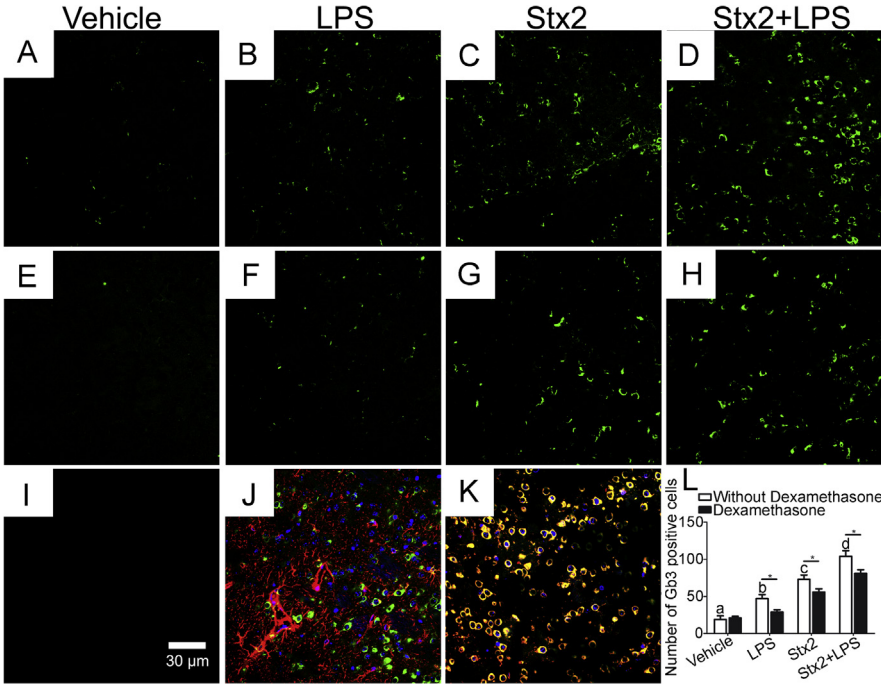

Fig. 8. Changes in the expression of Gb3. Treatment without Dexamethasone (A–D); treatment with Dexamethasone (E–H). Micrographs show immunofluorescence staining for Gb3 in neurons with anti-Gb3. (A, E) Vehicle; (B, F) LPS; (C, G) Stx2; (D, H) Stx2 + LPS. (I) Negative control by not adding the primary antibody (I). Merge between an immunofluorescence micrograph for Gb3 (green), another micrograph for GFAP (red) and Hoechst one (blue) showing that Gb3 is localized in neurons and not in astrocytes (J). Merge between an immunofluorescence micrograph for NeuN and another micrograph for Gb3 showing colocalization for both, in yellow (K) Dexamethasone decreases the number of Gb3-immunopositive neurons (L). Different letters (a, b, c or d) above the columns indicate a significant difference between the four different e.v.-treated groups without Dexamethasone treatment ($p \leqslant 0.05$). *Significant difference between the Dexamethasone-treated group with the same e.v.-treated group but without Dexamethasone ($p \leqslant 0.05$). Data are mean ± SEM. The scale bar in I applies to all micrographs. (For interpretation of the references to color in this figure legend, the reader is referred to the web version of this article.)

and second that anti-LPS antibodies belonging to the O157:H7 serotype have been found in the serum of HUS patients with clinical evidence of endotoxemia (Koster et al., 1978; Bitzan et al., 1991). Therefore, the LPS contribution on HUS pathogenicity should be included on animal models of HUS-derived encephalopthy.

The intact conservation of the microcalix from BBB endothelial cells is important to maintain not only the normal function of the microvasculature, but also the proper homeostasis of parenchymal brain cells. In contrast, an abnormal permeability can lead to neuronal stress and even death (Henry and Duling, 1999; Vink and Duling, 2000; Nieuwdorp et al., 2005). In the present work the discontinuity observed on endothelial glycocalyx expression, supports the fact that Stx2 breaks the BBB causing abnormal permeability. Therefore, the toxin succeeds to penetrate the striatal parenchyma. Once the toxin is inside the parenchyma it may damage the cells that modulate motor functions.

As the number of positive glycocalyx-particles bound to fluorescence lectins was increased by the toxins, it was possible to suppose that this event could be the cause of an angiogenic process. Therefore, immunofluorescence to detect VEGF was performed to test whether an angiogenic process was occurred. The results proved that this was not the case as VEGF immunoexpression was decreased concomitantly with glycocalyx discontinuity in endothelial cells following toxins treatments. VEGF is relevant to neurons as it has been reported that VEGF enhanced neuronal survival, neurite outgrowth and maturation under stress situations (Silverman et al., 1999; Rosenstein et al., 2003; Khaibullina et al., 2004). On the other hand, it has been found that VEGF expression decreased after Stx incubation in culture (Psotka et al., 2009). In addition recent reports have indicated that the loss of VEGF caused neurodegeneration (Rosenstein et al., 2003), an event that it may have contributed to the observed neuronal loss in our work.

The contribution of LPS in the encephalopathy driven by Stx2 resulted to enhance even more the BBB permeability caused by the Stx2 alone. This is very consistent with previous reports by which the co-administration of Stx and LPS resulted in a more severe hemorrhage compared with Stx2 alone (Sugatani et al., 2000). On the other hand the Dexamethasone treatment succeeded to partially restore the BBB, conserved endothelial cell integrity and it was neuroprotectant. This drug possesses and anti-inflammatory effect. Its pharmacological action includes the reduction of cytokines and the increased expression of occludin's tight junction proteins on brain endothelial basolateral cell membranes (Liu et al., 2000; Forster et al., 2006; Goldstein et al., 2007) making them less permeable. In this sense it is possible that Dexamethasone prevents the passage of the toxins to the striatal parenchyma from the blood and also a decrease in the expression of cytokines as TNFα and IL-1β, contributing to the reduction of neuronal damage.

In our model, we demonstrated that at least two distinct cell populations have shown changes in the expression of cytoskeletal proteins, astrocytes and neurons (Goldstein et al., 2007; Boccoli et al., 2008; Pinto et al., 2013). The astrocytes constitute the neurovascular unit and also the BBB through their endfeet. They play many functions as the regulation of blood flow, homeostasis of extracellular fluid, ions and transmitters, energy provision, and regulation of synapse function (Sofroniew and Vinters, 2010), and react in response to all types of insults (Little and O'Callagha, 2001) such as ischemia, neurodegenerative or infective diseases and trauma (Jacob et al., 2007; Pekny et al., 2007), in a phe-

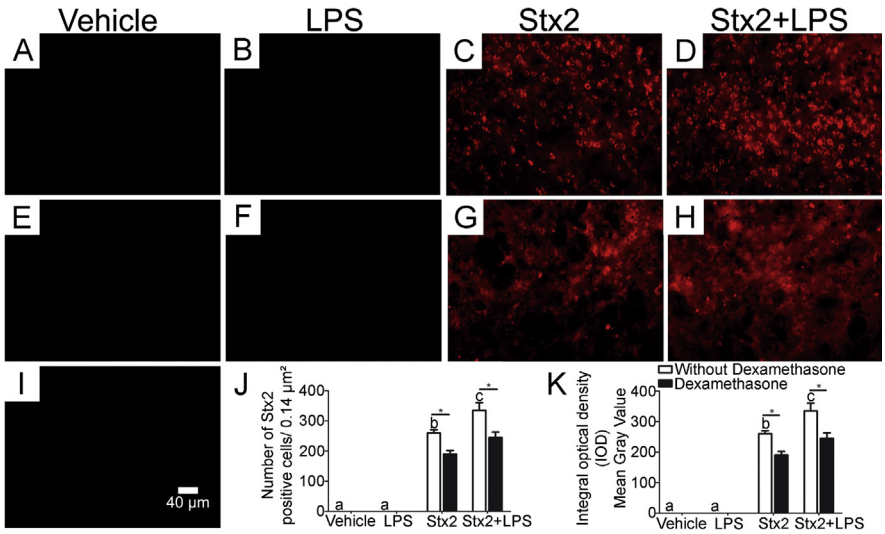

Fig. 9. Immunolocalization and quantification of Stx2. Treatment without Dexamethasone (A–D); treatment with Dexamethasone (E–H). Micrographs show immunofluorescence staining for Stx2 striatal cells with an anti-Stx2 antibody. (A, E) vehicle; (B, F) LPS; (C, G) Stx2; (D, H) Stx2 + LPS. Negative control by not adding the primary antibody (I). Dexamethasone decreases the number of Stx2-immunopositive cells (J). Dexamethasone decreases the intensity levels of endocytized Stx2 (K). Different letters (a, b or c) above the columns indicate a significant difference between the four different e.v.-treated groups without Dexamethasone treatment ($p \leqslant 0.05$). *Significant difference between the Dexamethasone-treated group with the same e.v.-treated group but without Dexamethasone ($p \leqslant 0.05$). Data are mean ± SEM. The scale bar in I applies to all micrographs.

nomenon called reactive astrocytes. At this state the expression of GFAP is upregulated, the cell is hypertrophied, and cell proliferation and pro- or anti-inflammatory effects occur (Sofroniew and Vinters, 2010). Many types of different molecules can lead to reactive astrogliosis like TNF-α, INFγ, LPS, etc. In CNS injury, reactive astrocytes are responsible for many beneficial functions, including BBB repair, neural protection and restricting the spread of inflammatory cells, and infection (Sofroniew and Vinters, 2010).

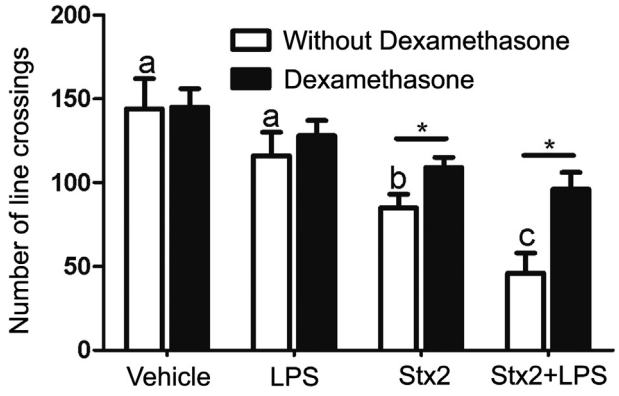

Fig. 10. Open field test. Mice were treated either with vehicle, LPS, Stx2 or Stx2 + LPS. Different letters (a, b or c) above the columns indicate a significant difference between the four different e.v.-treated groups without Dexamethasone treatment ($p \leqslant 0.05$). *Significant difference between the Dexamethasone-treated group with the same e.v.-treated group but without Dexamethasone ($p \leqslant 0.05$). Data are mean ± SEM.

On the contrary, neurons showed a decrease in the immunoexpression of MAP2, a structural microtubule-binding protein that binds to tubulin polymers and contribute to the regulation of their functions on neurite formation and maintenance. The MAP2 family comprises an abundant group of heat-stable proteins in the mammalian central nervous system and may have an important role in neurite outgrowth and in neuronal plasticity (Sanchez et al., 2000). Loss of MAP2 expression was reported as an early indicator of ischemia-induced neurodegeneration (Ballough et al., 1995; Raley-Susman and Murata, 1995; Folkerts et al., 1998; Schmidt-Kastner et al., 1998). The activation of calpain mediated-proteolysis may be the cause of the observed decrease of MAP2 immunoexpression (Hicks et al., 1995; Arias et al., 1997; Minana et al., 1998). As it is known, cytoskeleton disruption by proteolysis is one of the first signs of cell degeneration (Cotran et al., 1999). However, future experiments should be done to confirm this hypothesis.

In light of presented data neurodegeneration was determined using an immunofluorescence assay against NeuN. Direct damage to neurons by Stx2 has been previously demonstrated (Goldstein et al., 2007) probably through its Gb3 receptor (Tironi-Farinati et al., 2010). NeuN is a Fox-3 gene product, a member of the Fox-1 gene family of splicing factors that serves as a regulator of alternative splicing of pre-mRNA. Its expression is restricted to neurons and its subcellular localization is used to diagnose early events of neurodegeneration (Kim et al., 2009; Dent et al., 2010). Co-administration of both toxins increased the number of damaged neurons compared to the number of damaged neurons when Stx2 was administered alone. In the present work it was demonstrated that Dexamethasone protected approximately 50% of the neurons when it was challenged against the treatment of Stx2 together with LPS (Fig. 6K). In light of this result proinflammatory cytokines could play an important role in neurodegenerative processes, but other endogenous harmful agents may not be discarded.

In order to characterize motor activity in mice subjected to the treatment of Stx2 and/or LPS the Open Field assay was used to test, for the first time, the integrity of piramidal and extra-piramidal pathways. Animals experienced akinetic symptoms probably due to changes in the content of dopamine from the nigrostriatal pathway. The significant decrease on the motor activity by both toxins is consistent with the observed cell damage in the basal ganglia. Significant damage to other motor brain areas was also determined such the motor cortex (Pinto et al., 2013), supporting

the fact that Stx2 alters the motor system. Similar findings were observed in patients (Upadhyaya et al., 1980; Sheth et al., 1986; Hahn et al., 1989; Tironi-Farinati et al., 2010). Finally, Dexamethasone treatment partially reversed motor activity deficit suggesting the involvement of pro-inflammatory mechanisms that occurs during the encephalopathy.

In summary the present study demonstrated the cytotoxic effect of Stx2 in the microvasculature, astrocytes and neurons of mice striatum. LPS contribution enhances its deleterious effects. All these events were closely related with motor behavioral alterations. Finally, Dexamethasone treatment resulted to reverse the pathological condition produced by the toxins and may be beneficial to ameliorate the negative pathogen effects in the brain.

CONCLUSIONS

Outbreaks by intoxication with EHEC frequently occur worldwide in north and south hemispheres, and mortality rate caused by HUS rises dramatically when the CNS is involved. Furthermore, the inflammatory implication in the striatum has not been integrally investigated, nor a murine model that intends to mimic human clinical symptoms has not been widely established as a valuable tool. The current study integrates for the first time physiological, structural and behavioral data in the striatum. It demonstrates that sublethal Stx2 breaks the Blood–Brain Barrier and damages the microvasculature, astrocytes and neurons, and that LPS enhances its deleterious effects. These events lead to motor deficits while the Dexamethasone treatment reverses the pathological condition produced by the toxins. Our results show that anti-inflammatory therapeutics may be beneficial to treat the observed alterations of the neurovascular unit by reducing the cell damage and therefore to ameliorate motor disturbances found in patients.

DECLARATION OF INTEREST

The authors have declared that no competing interests exist.

AUTHOR CONTRIBUTION STATEMENT

Conceived and designed the experiments: Alipio Pinto and Jorge Goldstein. Performed the experiments: Alipio Pinto, Adriana Cangelosi, Patricia Geoghegan and Jorge Goldstein. Analyzed the data: Alipio Pinto and Jorge Goldstein. Contributed, reagents, materials, analysis tools: Alipio Pinto, Adriana Cangelosi, Patricia Geoghegan and Jorge Goldstein. Wrote the manuscript: Alipio Pinto and Jorge Goldstein.

FUNDING INFORMATION

These studies were supported by CONICET (National Research Council, Argentina) Grant PIP 112-201101-00901 and Universidad de Buenos Aires (UBA) grant UBACYT 20020120100353BA to J. Goldstein.

REFERENCES

Alexander C, Rietschel ET (2001) Bacterial lipopolysaccharides and innate immunity. J Endotoxin Res 7:167–202.

Arias C, Arrieta I, Massieu L, Tapia R (1997) Neuronal damage and MAP2 changes induced by the glutamate transport inhibitor dihydrokainate and by kainate in rat hippocampus *in vivo*. Exp Brain Res 116:467–476.

Bale Jr JF, Brasher C, Siegler RL (1980) CNS manifestations of the hemolytic-uremic syndrome. Relationship to metabolic alterations and prognosis. Am J Dis Child 134:869–872.

Ballough GP, Martin LJ, Cann FJ, Graham JS, Smith CD, Kling CE, Forster JS, Phann S, Filbert MG (1995) Microtubule-associated protein 2 (MAP-2): a sensitive marker of seizure-related brain damage. J Neurosci Methods 61:23–32.

Bielaszewska M, Mellmann A, Zhang W, Kock R, Fruth A, Bauwens A, Peters G, Karch H (2011) Characterisation of the Escherichia coli strain associated with an outbreak of haemolytic uraemic syndrome in Germany, 2011: a microbiological study. Lancet Infect Dis 11:671–676.

Bitzan M, Moebius E, Ludwig K, Muller-Wiefel DE, Heesemann J, Karch H (1991) High incidence of serum antibodies to *Escherichia coli* O157 lipopolysaccharide in children with hemolytic-uremic syndrome. J Pediatr 119:380–385.

Boccoli J, Loidl CF, Lopez-Costa JJ, Creydt VP, Ibarra C, Goldstein J (2008) Intracerebroventricular administration of Shiga toxin type 2 altered the expression levels of neuronal nitric oxide synthase and glial fibrillary acidic protein in rat brains. Brain Res 1230:320–333.

Brasher C, Siegler RL (1981) The hemolytic-uremic syndrome. West J Med 134:193–197.

Cimolai N, Morrison BJ, Carter JE (1992) Risk factors for the central nervous system manifestations of gastroenteritis-associated hemolytic-uremic syndrome. Pediatrics 90:616–621.

Cotran, R.S., Kuma, r V., Collins, T. (1999) Cellular adaptations, cell injury, and cell death, in pathologic basis of disease. Robbins. Philadelphia, 9th edition, Pennsylvania: W.B. Saunders Company, pp 31–32.

del Valle J, Camins A, Pallas M, Vilaplana J, Pelegri C (2008) A new method for determining blood–brain barrier integrity based on intracardiac perfusion of an Evans Blue-Hoechst cocktail. J Neurosci Methods 174:42–49.

Dent MA, Segura-Anaya E, Alva-Medina J, Aranda-Anzaldo A (2010) NeuN/Fox-3 is an intrinsic component of the neuronal nuclear matrix. FEBS Lett 584:2767–2771.

Ferreira T and Rasband WS (2010–2012) ImageJ User Guide — IJ 1.46, imagej.nih.gov/ij/docs/guide/.

Folkerts MM, Berman RF, Muizelaar JP, Rafols JA (1998) Disruption of MAP-2 immunostaining in rat hippocampus after traumatic brain injury. J Neurotrauma 15:349–363.

Forster C, Waschke J, Burek M, Leers J, Drenckhahn D (2006) Glucocorticoid effects on mouse microvascular endothelial barrier permeability are brain specific. J Physiol 573:413–425.

Frank C, Werber D, Cramer JP, Askar M, Faber M, Heiden M, Bernard H, Fruth A, Prager R, Spode A, Wadl M, Zoufaly A, Jordan S, Kemper MJ, Follin P, Muller L, King LA, Rosner B, Buchholz U, Stark K, Krause G (2011) Epidemic profile of Shiga-toxin-producing Escherichia coli O104:H4 outbreak in Germany. N Engl J Med 365:1771–1780.

Fujii J, Kinoshita Y, Kita T, Higure A, Takeda T, Tanaka N, Yoshida S (1996) Magnetic resonance imaging and histopathological study of brain lesions in rabbits given intravenous verotoxin 2. Infect Immun 64:5053–5060.

Gianantonio CA, Vitacco M, Mendilaharzu F, Gallo GE, Sojo ET (1973) The hemolytic-uremic syndrome. Nephron 11:174–192.

Goldstein J, Loidl CF, Creydt VP, Boccoli J, Ibarra C (2007) Intracerebroventricular administration of Shiga toxin type 2 induces striatal neuronal death and glial alterations: an ultrastructural study. Brain Res 1161:106–115.

Grisaru S, Midgley JP, Hamiwka LA, Wade AW, Samuel SM (2011) Diarrhea-associated hemolytic uremic syndrome in southern

Alberta: a long-term single-centre experience. Paediatr Child Health 16:337–340.
Hahn JS, Havens PL, Higgins JJ, O'Rourke PP, Estroff JA, Strand R (1989) Neurological complications of hemolytic-uremic syndrome. J Child Neurol 4:108–113.
Hamano S, Nakanishi Y, Nara T, Seki T, Ohtani T, Oishi T, Joh K, Oikawa T, Muramatsu Y, Ogawa Y, et al. (1993) Neurological manifestations of hemorrhagic colitis in the outbreak of Escherichia coli O157:H7 infection in Japan. Acta Paediatr 82:454–458.
Henry CB, Duling BR (1999) Permeation of the luminal capillary glycocalyx is determined by hyaluronan. Am J Physiol 277: H508–514.
Hicks RR, Smith DH, McIntosh TK (1995) Temporal response and effects of excitatory amino acid antagonism on microtubule-associated protein 2 immunoreactivity following experimental brain injury in rats. Brain Res 678:151–160.
Jacob A, Hensley LK, Safratowich BD, Quigg RJ, Alexander JJ (2007) The role of the complement cascade in endotoxin-induced septic encephalopathy. Lab Invest 87:1186–1194.
Karmali MA (2004) Infection by Shiga toxin-producing *Escherichia coli*: an overview. Mol Biotechnol 26:117–122.
Karmali MA, Petric M, Lim C, Fleming PC, Arbus GS, Lior H (1985) The association between idiopathic hemolytic uremic syndrome and infection by verotoxin-producing *Escherichia coli*. J Infect Dis 151:775–782.
Khaibullina AA, Rosenstein JM, Krum JM (2004) Vascular endothelial growth factor promotes neurite maturation in primary CNS neuronal cultures. Brain Res Dev Brain Res 148:59–68.
Kim KK, Adelstein RS, Kawamoto S (2009) Identification of neuronal nuclei (NeuN) as Fox-3, a new member of the Fox-1 gene family of splicing factors. J Biol Chem 284:31052–31061.
Kita E, Yunou Y, Kurioka T, Harada H, Yoshikawa S, Mikasa K, Higashi N (2000) Pathogenic mechanism of mouse brain damage caused by oral infection with Shiga toxin-producing *Escherichia coli* O157:H7. Infect Immun 68:1207–1214.
Koster F, Levin J, Walker L, Tung KS, Gilman RH, Rahaman MM, Majid MA, Islam S, Williams Jr RC (1978) Hemolytic-uremic syndrome after shigellosis. Relation to endotoxemia and circulating immune complexes. N Engl J Med 298:927–933.
Little AR, O'Callagha JP (2001) Astrogliosis in the adult and developing CNS: is there a role for proinflammatory cytokines? Neurotoxicology 22:607–618.
Liu CC, Chien CH, Lin MT (2000) Glucocorticoids reduce interleukin-1 concentration and result in neuroprotective effects in rat heatstroke. J Physiol 527(Pt 2):333–343.
Louise CB, Obrig TG (1992) Shiga toxin-associated hemolytic uremic syndrome: combined cytotoxic effects of shiga toxin and lipopolysaccharide (endotoxin) on human vascular endothelial cells *in vitro*. Infect Immun 60:1536–1543.
Mazzetti S, Frigerio S, Gelati M, Salmaggi A, Vitellaro-Zuccarello L (2004) Lycopersicon esculentum lectin: an effective and versatile endothelial marker of normal and tumoral blood vessels in the central nervous system. Eur J Histochem 48:423–428.
Minana MD, Montoliu C, Llansola M, Grisolia S, Felipo V (1998) Nicotine prevents glutamate-induced proteolysis of the microtubule-associated protein MAP-2 and glutamate neurotoxicity in primary cultures of cerebellar neurons. Neuropharmacology 37:847–857.
Mizuguchi M, Sugatani J, Maeda T, Momoi T, Arima K, Takashima S, Takeda T, Miwa M (2001) Cerebrovascular damage in young rabbits after intravenous administration of Shiga toxin 2. Acta Neuropathol 102:306–312.
Nieuwdorp M, Meuwese MC, Vink H, Hoekstra JB, Kastelein JJ, Stroes ES (2005) The endothelial glycocalyx: a potential barrier between health and vascular disease. Curr Opin Lipidol 16:507–511.
Obata F (2010) Influence of *Escherichia coli* shiga toxin on the mammalian central nervous system. Adv Appl Microbiol 71:1–19.
Parma YR, Chacana PA, Roge A, Kahl A, Cangelosi A, Geoghegan P, Lucchesi PM, Fernandez-Miyakawa ME (2011) Antibodies anti-Shiga toxin 2 B subunit from chicken egg yolk: isolation, purification and neutralization efficacy. Toxicon 58:380–388.
Pekny M, Wilhelmsson U, Bogestal YR, Pekna M (2007) The role of astrocytes and complement system in neural plasticity. Int Rev Neurobiol 82:95–111.
Pinto A, Jacobsen M, Geoghegan PA, Cangelosi A, Cejudo ML, Tironi-Farinati C, Goldstein J (2013) Dexamethasone rescues neurovascular unit integrity from cell damage caused by systemic administration of shiga toxin 2 and lipopolysaccharide in mice motor cortex. PLoS One 8:e70020.
Plunkett 3rd G, Rose DJ, Durfee TJ, Blattner FR (1999) Sequence of Shiga toxin 2 phage 933W from *Escherichia coli* O157:H7: Shiga toxin as a phage late-gene product. J Bacteriol 181:1767–1778.
Proulx F, Seidman EG, Karpman D (2001) Pathogenesis of Shiga toxin-associated hemolytic uremic syndrome. Pediatr Res 50:163–171.
Psotka MA, Obata F, Kolling GL, Gross LK, Saleem MA, Satchell SC, Mathieson PW, Obrig TG (2009) Shiga toxin 2 targets the murine renal collecting duct epithelium. Infect Immun 77:959–969.
Raley-Susman KM, Murata J (1995) Time course of protein changes following *in vitro* ischemia in the rat hippocampal slice. Brain Res 694:94–102.
Rivas M, Caletti MG, Chinen I, Refi SM, Roldan CD, Chillemi G, Fiorilli G, Bertolotti A, Aguerre L, Sosa Estani S (2003) Home-prepared hamburger and sporadic hemolytic uremic syndrome, Argentina. Emerg Infect Dis 9:1184–1186.
Rosenstein JM, Mani N, Khaibullina A, Krum JM (2003) Neurotrophic effects of vascular endothelial growth factor on organotypic cortical explants and primary cortical neurons. J Neurosci 23:11036–11044.
Sanchez C, Diaz-Nido J, Avila J (2000) Phosphorylation of microtubule-associated protein 2 (MAP2) and its relevance for the regulation of the neuronal cytoskeleton function. Prog Neurobiol 61:133–168.
Scheutz F, Nielsen EM, Frimodt-Moller J, Boisen N, Morabito S, Tozzoli R, Nataro JP, Caprioli A (2011) Characteristics of the enteroaggregative Shiga toxin/verotoxin-producing *Escherichia coli* O104:H4 strain causing the outbreak of haemolytic uraemic syndrome in Germany, May to June 2011. Euro Surveill 16.
Schmidt-Kastner R, Zhao W, Truettner J, Belayev L, Busto R, Ginsberg MD (1998) Pixel-based image analysis of HSP70, GADD45 and MAP2 mRNA expression after focal cerebral ischemia: hemodynamic and histological correlates. Brain Res Mol Brain Res 63:79–97.
Sheth KJ, Swick HM, Haworth N (1986) Neurological involvement in hemolytic-uremic syndrome. Ann Neurol 19:90–93.
Silverman WF, Krum JM, Mani N, Rosenstein JM (1999) Vascular, glial and neuronal effects of vascular endothelial growth factor in mesencephalic explant cultures. Neuroscience 90:1529–1541.
Sofroniew MV, Vinters HV (2010) Astrocytes: biology and pathology. Acta Neuropathol 119:7–35.
Sugatani J, Igarashi T, Munakata M, Komiyama Y, Takahashi H, Komiyama N, Maeda T, Takeda T, Miwa M (2000) Activation of coagulation in C57BL/6 mice given verotoxin 2 (VT2) and the effect of co-administration of LPS with VT2. Thromb Res 100:61–72.
Tapper D, Tarr P, Avner E, Brandt J, Waldhausen J (1995) Lessons learned in the management of hemolytic uremic syndrome in children. J Pediatr Surg 30:158–163.
Tironi-Farinati C, Loidl CF, Boccoli J, Parma Y, Fernandez-Miyakawa ME, Goldstein J (2010) Intracerebroventricular Shiga toxin 2 increases the expression of its receptor globotriaosylceramide and causes dendritic abnormalities. J Neuroimmunol 222:48–61.
Tironi-Farinati C, Geoghegan PA, Cangelosi A, Pinto A, Loidl CF, Goldstein J (2013) A translational murine model of sub-lethal intoxication with Shiga toxin 2 reveals novel ultrastructural findings in the brain striatum. PLoS One 8:e55812.
Upadhyaya K, Barwick K, Fishaut M, Kashgarian M, Siegel NJ (1980) The importance of nonrenal involvement in hemolytic-uremic syndrome. Pediatrics 65:115–120.

Vink H, Duling BR (2000) Capillary endothelial surface layer selectively reduces plasma solute distribution volume. Am J Physiol Heart Circ Physiol 278:H285–289.

Zhang H, Peterson JW, Niesel DW, Klimpel GR (1997) Bacterial lipoprotein and lipopolysaccharide act synergistically to induce lethal shock and proinflammatory cytokine production. J Immunol 159:4868–4878.

(Received 20 July 2016, Accepted 21 December 2016)
(Available online 30 December 2016)